# Eigenvalue Signal Processing for Weather Radar Polarimetry: Removing the Bias induced by Antenna Coherent Cross-Channel Coupling

Michele Galletti[1], Dusan S. Zrnic[2], Frank Gekat[3], Peter Goelz[3]

[1] Brookhaven National Laboratory, United States Department of Energy, Environmental Sciences Department, 30 Bell Ave. Upton, NY 11973

[2] National Oceanic and Atmospheric Administration – National Severe Storms Laboratory 120 David L. Boren Blvd. Norman, OK 73072

[3] Selex Systems Integration GmbH, Raiffeisenstrasse 10, 41470, Neuss, Germany

Corresponding Author: mgalletti@bnl.gov

TEL: 1-631-344 5310 FAX: 1-631-344 2887

*Abstract*— We present a novel digital signal processing procedure, named Eigenvalue Signal Processing (henceforth ESP), patented by the first author with Brookhaven Science Associates in 2013. The method enables the removal of the bias due to antenna coherent cross-channel coupling and is applicable in the LDR mode, the ATSR mode and the STSR orthogonal mode of weather radar measurements. In this work we focus on the LDR mode and consider copolar reflectivity at horizontal transmit ($Z_{HH}$), cross-polar reflectivity at horizontal transmit ($Z_{VH}$), linear depolarization ratio at horizontal transmit ($LDR_H$) and degree of polarization at horizontal transmit ($DOP_H$). The eigenvalue signal processing method is substantiated by an experiment carried out in November 2012 using C-band weather radar with a parabolic reflector located at the Selex Systems Integration (Selex SI) facilities in Neuss, Germany. The experiment involved comparison of weather radar measurements taken 1.5 minutes apart in two hardware configurations, namely with cross-coupling on (cc-on) and cross-coupling off (cc-off). It is experimentally demonstrated that eigenvalue-derived variables are invariant with respect to antenna coherent cross-channel coupling. This property had to be expected, since the eigenvalues of the Coherency matrix are SU(2) invariant.

***Keywords: polarimetric phased array weather radar, Coherency matrix, Covariance matrix, eigenvalues, cross-polar correlation coefficient, linear depolarization ratio, degree of polarization at horizontal transmit, antenna radiation pattern, copolar radiation pattern, cross-polar radiation pattern, cross-channel coupling.***

## I. INTRODUCTION

The development of polarimetric phased array weather radars is critical for the MPAR (Multi-function Phased Array Radar) mission. The major technological challenge in phased array weather radar polarimetry is attaining an acceptable cross-polar isolation between the H and V channels of the radar system. The present paper proposes Eigenvalue Signal Processing (ESP) to mitigate the problem of antenna cross-polarization isolation, and is potentially suitable for implementation in polarimetric phased array antennas, but also in conventional parabolic reflectors. A prerequisite for the understanding of the present paper is reference [1]. The Degree of Polarization at Horizontal/Vertical transmit is the theoretical centerpiece that permits the derivation of unbiased estimates of Reflectivity Z, Linear Depolarization Ratio LDR, and Differential Reflectivity $Z_{DR}$. The strength of the ESP approach resides in the fact that bias correction is obtained without knowing the actual amount of antenna cross-polar coupling. Indeed, the cross-polar correlation coefficients at horizontal and vertical transmit ($\rho_{xh}$ and $\rho_{xv}$) do provide an intrinsic measurement of antenna coherent cross-channel coupling (equation 66 in reference [1]), and the diagonalization of the Coherency matrices at horizontal and vertical polarizations automatically removes the bias from the two diagonal elements. This aspect is crucial: in the framework herein described, bias correction does not involve multiplying the retrieved scattering matrix with a "correction" matrix. The latter requires calibration to be performed on a beam-by-beam basis and, especially for large phased-arrays, it would render the engineering task daunting. Eigenvalue Signal Processing cannot retrieve unbiased scattering matrices but, under the reasonable assumption of target reflection symmetry [2], it can retrieve the unbiased Coherency matrices at horizontal and vertical polarization transmit, providing unbiased estimates for reflectivity Z, differential reflectivity $Z_{DR}$, and linear depolarization ratio LDR.

ESP hinges on three theoretical pillars:

1. The assumption that weather scatterers possess reflection symmetry [2], that is, they are non-canted and their intrinsic cross-polar correlation coefficients ($\rho_{xh}$ and $\rho_{xv}$) are equal to 0. We remind the reader that target reflection symmetry also underpins the choice of the STSR hybrid polarimetric architecture in present-day weather radars at S, C and X bands (e.g. NEXRAD) and is therefore considered to be a safe assumption [3].

2. The invariance of Degree of Polarization at Horizontal/Vertical transmit with respect to antenna coupling. An exhaustive analysis of $DOP_H$ is provided in reference [1]. Together with the previous point, $DOP_H$ invariance permits to derive an unbiased estimate for LDR, in the following named $LDR_{ESP}$.

3. The invariance of the trace of the Coherency matrix with respect to antenna coupling. This permits to derive an unbiased estimate for Z, in the following named $Z_{ESP}$. Applying the same procedure to the two Coherency matrices at H and V transmit yields an unbiased estimate for differential reflectivity $Z_{DR}$, in the following named $Z_{DR\_ESP}$.

From a superior viewpoint, there is only one theoretical principle underlying ESP: SU(2) transformations are an accurate mathematical representation of coherent antenna coupling acting on the antenna height spinor both on transit and receive (a derivation of the contravariant antenna height spinor and of the covariant wave spinor is presented in [4]). Since the eigenvalues of the Coherency matrix are SU(2) invariant, it follows that variables derived from the eigenvalues are also invariant. ESP theory provides an algebraic proof that the largest and smallest eigenvalues of the Coherency matrix correspond to the copolar and cross-polar powers measured by an antenna that is perfectly aligned with the principal axes of the illuminated distributed scatterer. In fact, Eigenvalue Signal Processing produces an alignment between the illuminated scatterers, (assumed to possess reflection symmetry and therefore characterized by intrinsic cross-polar correlation coefficients $\rho_{xh}$ and $\rho_{xv}$ equal to zero) and the antenna height spinor (assumed to be slightly tilted from the horizontal/vertical because of coherent cross-channel coupling). The alignment is produced by means of the diagonalization of the Coherency matrices at horizontal and vertical transmit $\mathbf{J_H}$ and $\mathbf{J_V}$. The source of the “misalignment” is ascribed to the coherent cross-polar power radiated by the antenna inducing positive non-zero cross-polar correlation coefficients.

In a loose analogy, Eigenvalue Signal Processing is for distributed (stochastic) scatterers what the Graves Power matrix theory is for single scatterers [5, 6]. In both cases the eigenvalues correspond to powers in the "aligned" reference frame.

Even though the present body of work originated within the synthetic aperture radar (SAR) polarimetry community [7-9], it has substantially departed from it, especially because all variables treated in the present paper (ESP variables) are obtained from the eigenvalues of the 2x2 Coherency matrices $\mathbf{J_H}$ and $\mathbf{J_V}$, whereas in the SAR polarimetry community focus is on eigenvalue- and eigenvector-derived variables of the 3x3 Covariance matrix **C** [8]. Operating on the 2x2 Coherency matrices involves SU(2) transformations, whereas operating on the 3x3 Covariance matrix involves SU(3) transformations. This aspect is fundamental and should not be overlooked. SU(2) describes a set of transformations that exactly corresponds to the set of polarization basis transformations, and therefore describes all the possible distortions imposed by the antenna on the radiated polarization state. This exact correspondence is such that SU(2)-derived eigenvalues (under the assumption of target reflection symmetry) exactly correspond to the antenna-unbiased copolar and cross-polar powers, as will be analytically illustrated in the following. The drawback of the eigen-analysis of the Coherency matrices is that, obviously, it cannot provide information about the 1,3 term of the 3x3 Covariance matrix, information traditionally encapsulated in the copolar correlation coefficient $\rho_{hv}$ and differential phase $\Psi_{DP}$. Eigen-analysis of the 3x3 Covariance matrix can however provide eigenvalue- and eigenvector-derived variables – scattering entropy H and the alpha angle $\alpha$ - which are good proxies for $\rho_{hv}$ and differential phase ($\Psi_{DP} = \Phi_{DP} + \delta_{co}$) respectively [10, 11]. In this case however, SU(3) spans a set of transformations that are larger (in the strict sense) than the set of polarization bases transformations [7], and the correspondence between eigen-variables (H, $\alpha$) and their traditional counterparts ($\rho_{hv}$ and $\Psi_{DP}$) is only approximate.

In the following, we will only focus on variables derived from the eigenvalues of the Coherency matrices $\mathbf{J_H}$ and $\mathbf{J_V}$. The ESP variables defined in the following ($Z_{ESP}$, $Z_{DR\_ESP}$, $LDR_{ESP}$) are antenna-unbiased replacements for standard radar meteorological variables obtained from the diagonal of the Covariance (Coherency) matrix: Reflectivity Z, Differential Reflectivity $Z_{DR}$ and Linear Depolarization Ratio LDR.

*A. Polarimetric Operating Modes and Orthogonal Waveforms*

Eigenvalue Signal Processing requires orthogonal polarization bases and is therefore applicable when the radar operates at LDR mode (Linear Depolarization Ratio mode), ATSR mode (Alternate Transmission Simultaneous Receive mode) or STSR orthogonal mode (Simultaneous Transmission Simultaneous Receive orthogonal mode - Fig. 1B and 1C), but it is not applicable at STSR hybrid mode (Simultaneous Transmission Simultaneous Receive hybrid mode Fig. 1A). LDR mode corresponds to horizontal polarization transmit, and simultaneous reception of H and V; ATSR mode corresponds to H transmit and simultaneous H and V receive, followed by V transmit and simultaneous H and V receive. STSR hybrid mode (Fig. 1A) corresponds to Simultaneous Transmission of H and V and Simultaneous Reception of H and V; here, hybrid indicates that the receive polarization basis is not copolar and cross-polar to the transmit polarization. STSR hybrid mode is the default choice for operational weather radars. STSR orthogonal corresponds to the simultaneous transmission and simultaneous reception of orthogonal H and V waveforms, with the capability of retrieving the four components of the scattering matrix **S** ($s_{hh}$, $s_{hv}$, $s_{vh}$, $s_{vv}$) in one pulse repetition time, instead of two as in the ATSR mode [12-14]. In this case, the word orthogonal refers to the two waveforms used to simultaneously excite the H and V channels, but may also refer to the fact that, using waveform diversity, the polarization basis in use is orthogonal even though the two pulses are radiated simultaneously. ESP is fully compatible with the use of waveform diversity in the radar system, since ESP relies on processing performed on the elements of the 2x2 Coherency matrices, that involve correlations of each of the two waveforms with itself, but do not involve correlations between the two different waveforms (the latter appearing only in the 1,3 term of the 3x3 Covariance matrix). In fig. 1B and 1C we consider two orthogonal waveforms, where the term orthogonal refers to their disjoint spectral support. Other definitions of orthogonal waveforms exist, for example phase-coded waveforms may be termed orthogonal even if their spectral support is overlapping. In any case, ESP is always compatible with waveform diversity, either spectrally disjoint, or phase-coded waveforms.

STSR orthogonal mode is looked at with increasing interest for phased array weather radar polarimetry, due to its property of lowering the isolation requirement on cross-polar isolation to the levels of the ATSR mode (requirement for ATSR mode is -25 dB, whereas for STSR hybrid it is around -45 dB [15]).

TABLE I. POLARIMETRIC ARCHITECTURES FOR WEATHER RADARS

| *Polarimetric Architecture* | *Standard Variables* | *ESP variables* |
|---|---|---|
| LDR mode (2-pol) | Z LDR | $Z_{ESP}$ $LDR_{ESP}$ |
| STSR hybrid mode (2-pol) | Z $Z_{DR}$ $\rho_{hv}$ KDP | None |
| ATSR mode (4-pol) | Z LDR $Z_{DR}$ $\rho_{hv}$ KDP | $Z_{ESP}$ $LDR_{ESP}$ $Z_{DR\_ESP}$ |
| STSR orthogonal mode (4-pol) | Z LDR $Z_{DR}$ $\rho_{hv}$ KDP | $Z_{ESP}$ $LDR_{ESP}$ $Z_{DR\_ESP}$ |

Besides lowering the requirement for antenna isolation to the levels of the ATSR mode, the use of orthogonal waveforms also permits the implementation of full polarimetry in half the scan time time as the ATSR mode or, equivalently, the same scan time as the STSR hybrid mode. As an application example, we consider two orthogonal waveforms WF1 and WF2 with disjoint spectral support such that their correlation is 0. Switching between the two waveforms in the H and V channels as indicated in Fig. 1C (STSR orthogonal 4-pol mode) allows one to retrieve all polarimetric variables in the same scan time as the STSR hybrid mode (Fig. 1A). The STSR orthogonal 4-pol mode (Fig. 1C) yields Z, $Z_{DR}$ and LDR at 0 lag (for which ESP is applicable) and $\rho_{hv}$ and KDP can be computed at 1 lag, as indicated in [16] and page 347 of [17].

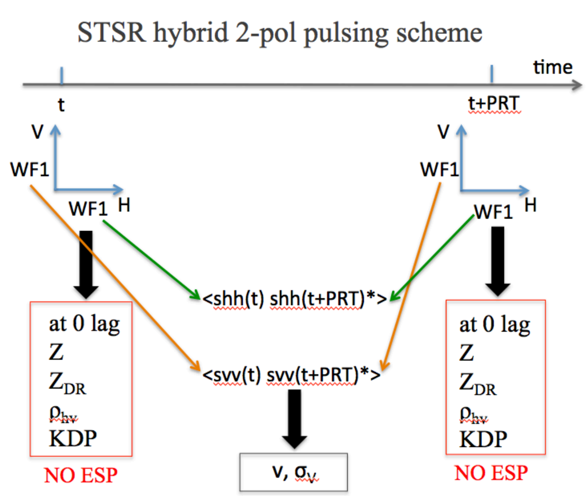


**Fig. 1A** STSR hybrid 2-pol mode. The same waveform (WF1) excites simultaneously the H and V channels, yielding estimates of Z, $Z_{DR}$, $\rho_{hv}$ and KDP at 0 lag. This operating mode is the standard in use for weather radar systems at S, C and X bands (e.g. NEXRAD). In this operating mode, ESP is not applicable, since transmit and receive polarization states are not orthogonal (hence the term hybrid).

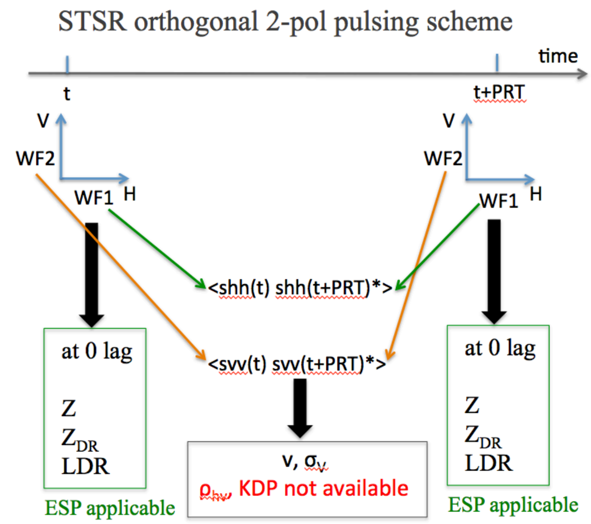


**Fig. 1B** STSR orthogonal 2-pol mode. Two orthogonal waveforms (WF1 and WF2) are used to excite the H and V channels. This yields simultanoeus measurements of Z, $Z_{DR}$ and LDR, yet prevents the estimation of $\rho_{hv}$ and KDP since the correlation of the two orthogonal waveforms, with disjoint spectral support, is 0 by definition (e.g. reference [12, 13]). ESP is applicable for the estimation of Z, $Z_{DR}$ and LDR.

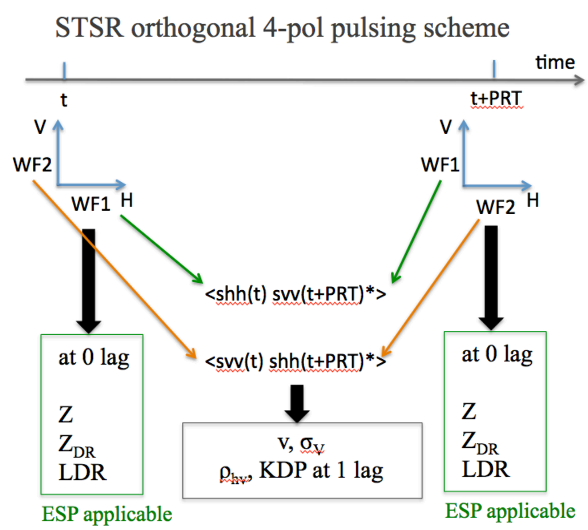


**Fig. 1C** STSR orthogonal 4-pol mode. Two orthogonal waveforms (WF1 and WF2) are used to excite the H and V channels by switching between Waveform 1 (WF1) and Waveform 2 (WF2) on a pulse-to-pulse basis. This operating mode yields Z, $Z_{DR}$ and LDR at 0 lag (for which ESP is applicable) and $\rho_{hv}$ and KDP at 1 lag [16, 17] in the same scan time as the STSR hybrid 2-pol pulsing scheme (Fig. 1A).

*B. Coherent versus Incoherent cross-polar power:a limitation in the effectiveness of ESP*

The unwanted cross-polar power radiated by any antenna can be split in two components: the incoherent cross-polar power, and the coherent cross-polar power [18]. The incoherent cross-polar power appears as a quad of perfectly symmetric offset lobes of the cross-polar antenna pattern, and is produced by the natural geometry of the electric field lines on the radiating surface of the antenna. The quad of offset cross-polar lobes is intrinsic to the parabolic reflectors as well as the microstrip patch antennas. When a cloud of spheres is illuminated (or, more generally, any target with reflection symmetry), such quad of offset lobes produces backscattered cross-polar power that is uncorrelated with the backscattered copolar power, and the cross-polar correlation coefficients ($\rho_{xh}$ and $\rho_{xv}$) are equal to zero. The bias in polarimetric variables induced by incoherent cross-polar power cannot be removed by eigenvalue signal processing. In the case of antennas characterized by the presence of significant incoherent cross-polar power, Eigenvalue Signal Processing cannot recover the polarimetric dynamic range corresponding to a well-isolated antenna. We will see in the ESP experiment in Section III that this is the case for the cc-off configuration: the antenna in use is characterized by slightly high minimum measurable LDR (~ - 26 dB) yet the cross-polar correlation coefficient $\rho_{xh}$ is still relatively low (~ 0.2 - 0.3), indicating the presence of incoherent cross-polar power.

The coherent cross-polar power appears whenever the 4 offset lobes are unbalanced (as may be the case in real parabolic reflectors, where the offset cross-polar lobes display different amplitudes and are not perfectly symmetric), or whenever cross-polar power is radiated axially, that is, along the bore sight of the antenna. Such coaxial cross-polar power is generated by a number of sources. In the case of parabolic reflectors, it can be generated by imperfections in the reflector surface, feed-horn misalignment, finite isolation of the orthomode transducer or scattering from the feed support struts. In the case of a planar phased array scanning off the horizontal and vertical planes, it is generated by the misalignment of the radiated field lines with respect to the local horizontal [19]. The coherent (coaxial) cross-polar power significantly increases the cross-polar correlation coefficients ($\rho_{xh}$ and $\rho_{xv}$), but the bias it introduces in the polarimetric variables can be removed by eigenvalue signal processing. We will see in Section III that this is the case of the cc-on configuration, where the bias in polarimetric variables induced by waveguide coupling can be corrected by applying ESP.

In general, minimum measurable LDR (in drizzle or warm clouds) is the optimal metric to establish the polarimetric quality of the antenna.

ESP can only correct for the coherent component of cross-polar power, and its effectiveness is established by the values (in drizzle or warm clouds) of the cross-polar correlation coefficients ($\rho_{xh}$ and $\rho_{xv}$). The cross-polar correlation coefficients do provide information about the spatial structure of cross-polar power, that is, low cross-polar correlation coefficeints (< 0.2 - 0.3) indicate that incoherent cross-polar power is dominant (quad of offset lobes), whereas high cross-polar correlation coefficients (> 0.7 - 0.8) indicate that coherent (coaxial) cross-polar power is dominant, as explained in [1]. Therefore, ESP always improves the performance of the antenna, but the extent of the improvement is driven by the coherent vs. incoherent nature of cross-polar power. Specifically, ESP only removes the coherent component of cross-polar power, and its application may yield different results on different antennas, depending on the coherent power level of the antenna in use. For example, for the cc-off case illustrated in the following, where incoherent cross-pol power dominates, the improvement brought by ESP is small. The effects of ESP are also unnoticeable in well-isolated antennas with low LDR (< -30 dB) and low $\rho_{xh}$ (< 0.3) in drizzle/light rain, like the recently modified CSU-CHILL [20] or the KOUN WSR-88D prototype at NSSL. For example, the effects of ESP on the KOUN radar are essentially undetectable: in that case minimum measurable LDR (drizzle/light rain) is around -33 dB, and the corresponding $\rho_{xh}$ is around 0.2 [21], indicating the presence of only a very small amount of incoherent cross-polar power (quad of offset lobes).

So, if incoherent cross-polar power (quad of offset lobes - low $\rho_{xh}$ and $\rho_{xv}$) is dominant, Eigenvalue Signal Processing does not significantly improve antenna isolation, since the effect of cross-polar power does not correspond to an SU(2) rotation of the radiated covariant wave spinor [4]. If coaxial cross-polar power is dominant (large cross-polar correlation coefficients when drizzle or warm cloud droplets are illuminated), the application of ESP permits to correct Z, LDR and $Z_{DR}$ for the bias induced by poor antenna isolation. This result has important implications in weather radar polarimetry, both for parabolic reflectors and for phased-array antennas.

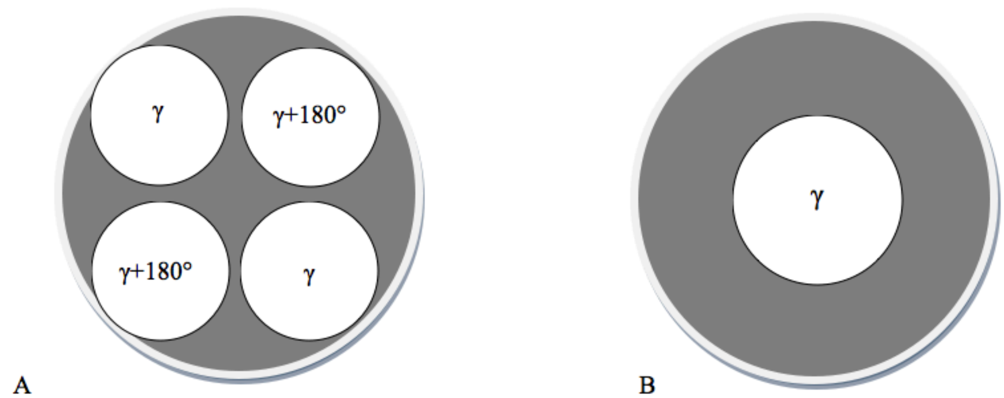


**Fig.2** Idealized antenna cross-polar patterns corresponding to incoherent cross-polar power (A), dominant in parabolic reflectors, and coherent cross-polar power (B), dominant in planar phased array antennas.

## II. Theoretical Background

### A. Coherency matrix

In this paragraph we reprise the concepts exposed in [1]. Weather radars at LDR mode measure the Coherency matrix at horizontal polarization transmit ($\mathbf{J}_H$), a matrix with 4 degrees of freedom. Note that this matrix is the upper left 2×2 minor of the backscatter covariance matrix in [22].

$$\mathbf{J}_H = \begin{bmatrix} \langle |s_{hh}|^2 \rangle & \langle s_{hh}^* s_{vh} \rangle \\ \langle s_{hh} s_{vh}^* \rangle & \langle |s_{vh}|^2 \rangle \end{bmatrix} \quad (1)$$

From the Coherency matrix, radar variables are evaluated. From the two degrees of freedom on the diagonal, we can extract copolar reflectivity ($Z_{HH}$) cross-polar reflectivity ($Z_{VH}$) and the linear depolarization ratio ($LDR_H$)

$$Z_{HH} \propto \langle |s_{hh}|^2 \rangle \quad (2)$$

$$Z_{VH} \propto \langle |s_{vh}|^2 \rangle \quad (3)$$

$$\mathrm{LDR_H} = \frac{\langle |s_{vh}|^2 \rangle}{\langle |s_{hh}|^2 \rangle}$$

(4)

Reflectivity is proportional to the power backscattered at horizontal polarization, the linear depolarization ratio is representative of the target-induced coupling between copolar (horizontal) and cross-polar (vertical) channels. The two degrees of freedom on the off-diagonal term are captured by the cross-polar correlation coefficient ($\rho_{xh}$) and the cross-polar phase $\psi_{xh}$ (propagation $\Phi_{xh}$ plus back scatter $\delta_{xh}$).

$$\rho_{xh} = \frac{|\langle s_{hh}^* s_{vh} \rangle|}{\sqrt{\langle |s_{hh}|^2 \rangle \langle |s_{vh}|^2 \rangle}}$$

(5)

$$\psi_{xh} = \Phi_{xh} + \delta_{xh} = \arg[\langle s_{hh}^* s_{vh} \rangle]$$

(6)

The cross-polar correlation coefficient ranges between 0 and 1, and is a normalized measure of the correlation between copolar and cross-polar signals. It is shown in [2] that cross-correlation departs from zero if and only if the target departs from reflection symmetry. Besides canted hydrometeors and ground clutter, aircrafts or other man-made objects can appear with positive, non-zero $\rho_{xh}$. The Coherency matrix $\mathbf{J_H}$ can be diagonalized to yield,

$$\mathbf{J}_H = \mathbf{U} \begin{bmatrix} \lambda_{H1} & 0 \\ 0 & \lambda_{H2} \end{bmatrix} \mathbf{U^{-1}}$$

(7)

Where $\lambda_{H1}$ is the largest eigenvalue and $\lambda_{H2}$ is the smallest eigenvalue of the Coherency matrix at horizontal transmit. The trace (corresponding to the total backscattered power) and the degree of polarization at horizontal transmit (corresponding to the ratio of completely polarized power to total power) are also derived from the eigenvalues.

$$\mathrm{Tr}\mathbf{J}_H = \lambda_{H1} + \lambda_{H2}$$

(8)

$$p_H = \frac{\lambda_{H1} - \lambda_{H2}}{\lambda_{H1} + \lambda_{H2}} = \sqrt{1 - \frac{4\det\mathbf{J}_H}{[\mathrm{Tr}\mathbf{J}_H]^2}}$$

(9)

These variables can also be expressed in terms of the entries of the Coherency matrix $\mathbf{J}_H$ as:

$$\mathrm{Tr}\mathbf{J}_H = \langle|s_{hh}|^2\rangle + \langle|s_{vh}|^2\rangle$$

(10)

$$p_H = \sqrt{1 - \frac{4\left[\langle|s_{hh}|^2\rangle\langle|s_{vh}|^2\rangle - \left|\langle s_{hh}s_{vh}^*\rangle\right|^2\right]}{[\langle|s_{hh}|^2\rangle + \langle|s_{vh}|^2\rangle]^2}}$$

(11)

The degree of polarization at horizontal transmit is related to $LDR_H$ and $\rho_{xh}$ by a fundamental identity in radar polarimetry, obtainable by simple algebraic manipulation of (11) [23, 24].

$$(1 - p_H^2) = \frac{4\,LDR_H}{[1 + LDR_H]^2}(1 - \rho_{xh}^2)$$

(12)

The diagonalization of the Coherency matrix nulls the cross-polar correlation coefficient $\rho_{xh}$, and the formula in (12) simplifies to

$$p_H = \frac{1 - LDR_H}{1 + LDR_H}$$

(13)

Algebraic manipulation of (13) and use of (9) permits to define the first ESP variable: $LDR_{H\_ESP}$

$$LDR_{H\_ESP} \equiv \frac{\lambda_{H2}}{\lambda_{H1}}$$

(14)

For an ideal antenna with no coherent cross-channel coupling (that is, an antenna that yields $\rho_{xh}=0$ and $\rho_{xv}=0$ when scatterers with reflection symmetry are illuminated), $LDR_{H\_ESP}$ is equal to $LDR_H$. In presence of coherent cross-channel coupling (that is, the antenna height spinor undergoes a small SU(2) rotation), $LDR_H$ is positively biased, whereas $LDR_{H\_ESP}$ is not significantly biased. In general, the following inequality holds as shown by a simple analysis of Fig.1a of reference [1].

$$\mathrm{LDR_{H\_ESP}} \leq \mathrm{LDR_H}$$

(15)

The next step is the realization that the trace of the Coherency matrix $\mathbf{J}_H$ is invariant for SU(2) transformations,

$$\mathrm{Tr}\mathbf{J}_H = \langle|s_{hh}|^2\rangle + \langle|s_{vh}|^2\rangle = Z_{HH}[1 + \mathrm{LDR_H}] = \lambda_{H1} + \lambda_{H2} = Z_{HH\_ESP}\left[1 + \mathrm{LDR_{H\_ESP}}\right]$$

(16)

This leads to the identification of the largest eigenvalue of the Coherency matrix ($\lambda_{H1}$) as the copolar (main) power received at LDR mode by an "aligned" antenna. This observation defines the second ESP variable:

$$Z_{HH\_ESP} \equiv \lambda_{H1}$$

(17)

Also, it follows from (16) that the copolar power received by a perfectly aligned antenna is always larger than its biased counterpart. Equality only holds when the cross-polar power is purely incoherent (perfect quad of offset cross-polar lobes).

$$Z_{HH\_ESP} \geq Z_{HH}$$

(18)

The antenna-unbiased cross-polar reflectivity (power received in the vertical channel for the case of horizontal polarization transmit) is given by the smallest eigenvalue of the Coherency matrix and is in general smaller than its biased counterpart:

$$Z_{VH\_ESP} \equiv \lambda_{H2}$$

(19)

$$Z_{VH\_ESP} \leq Z_{VH}$$

(20)

The development above suggests a precise physical meaning for the eigenvalues of the Coherency matrix, that is, the largest and the smallest eigenvalues correspond to the copolar and cross-polar powers respectively, as measured by an antenna whose antenna height spinor is perfectly aligned with the principal axes of the illuminated scatterers. The eigenvalues correspond to estimates of copolar and cross-polar powers that are unbiased by antenna coherent cross-polarization coupling, the unbiased depolarization ratio ($LDR_{H\_ESP}$) is given by their ratio.

*B. Covariance matrix*

If the weather radar operates at ATSR mode or STSR orthogonal mode, the development above can also be applied to the Coherency matrix at vertical polarization transmit $\mathbf{J}_V$.

$$\mathbf{J}_V = \begin{bmatrix} \langle|s_{vv}|^2\rangle & \langle s_{vv}^* s_{hv}\rangle \\ \langle s_{vv} s_{hv}^*\rangle & \langle|s_{hv}|^2\rangle \end{bmatrix} \tag{21}$$

In this case, copolar reflectivity, cross-polar reflectivity and linear depolarization ratio at vertical transmit are respectively defined as

$$Z_{VV} \propto \langle|s_{vv}|^2\rangle \tag{22}$$

$$Z_{HV} \propto \langle|s_{hv}|^2\rangle \tag{23}$$

$$LDR_V \equiv \frac{\langle|s_{hv}|^2\rangle}{\langle|s_{vv}|^2\rangle} \tag{24}$$

These can be corrected for the bias induced by antenna coherent cross-polarization simply by replacing them with their eigenvalue-derived counterparts:

$$Z_{VV\_ESP} \equiv \lambda_{V1} \tag{25}$$

$$Z_{HV\_ESP} \equiv \lambda_{V2} \tag{26}$$

$$\mathrm{LDR_{V\_ESP}} \equiv \frac{\lambda_{V2}}{\lambda_{V1}}$$

(27)

where $\lambda_{V1}$ and $\lambda_{V2}$ are respectively the largest and smallest eigenvalues of the Coherency matrix at vertical polarization transmit $\mathbf{J_V}$. The following inequalities hold for copolar reflectivity, cross-polar reflectivity and linear depolarization ratio:

$$\mathrm{Z_{VV\_ESP}} \geq \mathrm{Z_{VV}}$$

(28)

$$\mathrm{Z_{HV\_ESP}} \leq \mathrm{Z_{HV}}$$

(29)

$$\mathrm{LDR_{V\_ESP}} \leq \mathrm{LDR_V}$$

(30)

The last eigenvalue-derived variable is the bias-corrected replacement for differential reflectivity $Z_{DR}$, which can be obtained as the ratio of copolar reflectivities at horizontal and vertical transmit

$$\mathrm{Z_{DR\_ESP}} \equiv \frac{\mathrm{Z_{HH\_ESP}}}{\mathrm{Z_{VV\_ESP}}} \equiv \frac{\lambda_{H1}}{\lambda_{V1}}$$

(31)

The theory exposed in this Section permits the removal of the bias induced by antenna coherent cross-polarization coupling in power-like weather radar variables, specifically reflectivity Z, Linear Depolarization Ratio LDR and Differential Reflectivity $Z_{DR}$. The elegance of eigenvalue signal processing resides in the fact that bias correction does not require knowledge of the amount of cross-coupling, since the latter is intrinsically measured by the cross-polar correlation coefficients $\rho_{xh}$ and $\rho_{xv}$ and the diagonalization of the Coherency matrix automatically brings them to zero. It may have been noted that ESP does not provide replacements for variables derived from the 1,3 term of the covariance matrix, specifically the copolar correlation coefficient $\rho_{hv}$ and the specific differential phase KDP. This had to be expected, since ESP diagonalizes the 2x2 Coherency matrices $\mathbf{J_H}$ and $\mathbf{J_V}$, but does not involve the 1,3 term of the Covariance matrix. However, the copolar correlation coefficient ($\rho_{hv}$) and the specific differential phase (KDP), retreived in the ATSR mode and STSR orthogonal 4-pol mode, are not significantly affected by antenna cross-channel coupling [15]. At STSR orthogonal mode (both 2-pol and 4-pol), ESP is applicable for the retrieval of unbiased estimates of Z, $Z_{DR}$ and LDR, and at the same time it does not pose any constraint on the waveforms in use. In the case of the STSR hybrid mode, ESP is not applicable, because the receive polarization basis is not orthogonal to the transmit polarization basis. In Table II is a summary of radar meteorological variables and their eigenvalue-derived counterparts (far-right column). Even though not commonly used in radar meteorology, the degree of polarization and the trace of the coherency matrix (not listed in the table) are also eigenvalue-derived variables, and automatically enjoy the property of being robust against antenna cross-channel coupling.

TABLE II. ESP VARIABLES

| ***Name*** | ***Standard*** | ***ESP variables*** |
|---|---|---|
| Reflectivity at horizontal transmit | $Z_{HH}$ | $Z_{HH\_ESP}$ |
| Reflectivity at vertical transmit | $Z_{VV}$ | $Z_{VV\_ESP}$ |
| Linear Depolariz. Ratio at horizontal tx | $LDR_H$ | $LDR_{H\_ESP}$ |
| Linear Depolariz. Ratio at vertical tx | $LDR_V$ | $LDR_{V\_ESP}$ |
| Differential Reflectivity | $Z_{DR}$ | $Z_{DR\_ESP}$ |
| Copolar correlation coefficient | $\rho_{hv}$ | - |
| Specific Differential phase | KDP | - |

## III. EIGENVALUE SIGNAL PROCESSING EXPERIMENT

Eigenvalue Signal Processing was tested at LDR mode for $Z_{HH\_ESP}$, $Z_{VH\_ESP}$, $LDR_{H\_ESP}$ and $DOP_H$ in an experiment conducted on November 10th 2012 at the Selex Systems Integration facilities in Neuss, Nordrhein-Westfalen, Germany [25] at around 16:20 local time, when ground temperature was +11˚C. The data were collected with a modified METEOR 600C dual-polarization Doppler weather radar, that can implement both the STSR hybrid mode and the LDR mode [26]. The parabolic reflector C-band antenna (wavelength 5.3 cm, beamwidth 1.0˚ - for more specifications, antenna is indicated as CLP10 in [27]), acquired a PPI at 1.5˚ elevation in a weather event consisting of light stratiform rain, with the melting band visible as a low LDR ring around the radar at about 50 km distance. Pulse Repetition Frequency (PRF) was 1300 Hz, range resolution was 0.15 km, antenna azimuth velocity was 4.8˚/s, number of pulses per radial was 135 (collected over an angular interval of 0.5˚). The radar was operated at LDR mode, in two different configurations indicated with cc-on (red curve in the plots) and cc-off (blue and green curves in the plots). The cc-on acquisition was taken between 16:18:20 and 16:19:40 CET (Central European Time), whereas the cc-off acquisition was taken between 16:19:40 and 16:21:00 CET. The two acquisitions are spaced in time by about 1.5 minutes, and it can reasonably be assumed that the illuminated scatterers are the same. In the cc-off acquisition, the radar was operated in its standard LDR mode configuration, whereas in the cc-on acquisition, the detrimental effects of a poorly isolated antenna were simulated by disconnecting the V transmit waveguide and by injecting into the Tx port of the V circulator a signal sample extracted from the H transmit channel via a 20 dB coupler (Fig.3). By default, the radar is a hybrid design, that is, the transmitted pulse is split and fed with equal powers to the H and V waveguides, and reception  occurs simultaneously in the H and V channels (STSR hybrid mode). In order to implement the LDR mode, a remotely controlled mechanical waveguide switch redirects the full transmit power to the horizontal (H) polarization channel while the system still receives in both channels. In the following, we refer to this LDR mode hardware configuration as cross-coupling off (cc-off). To simulate antenna coupling, the system was modified as indicated in Fig. 3: the transmitter was directly connected to the H polarization transmit channel and to increase the cross-polarization of the system, a waveguide coupler (xpol coupler in Fig. 3) was inserted into the channel; the extracted pulse is then injected into the vertical (V) polarization channel via the waveguide switch. In the following, we refer to this hardware configuration as cross-coupling on (cc-on). This allows a quick on- and off-switching of the transmit cross-polarization. The difference in attenuation between the H and V antenna waveguide runs was H/V=0.75 dB. The coupling loss of the xpol signal was 22.4 dB. The described set-up simulates coherent (coaxial) cross-polar power on transmission only, since on reception the antenna is still acceptably isolated, and can be modelled with the following matrix multiplication

$$\mathbf{S}' = \mathbf{S}\,\mathbf{F} = \begin{bmatrix} s_{hh} & s_{hv} \\ s_{vh} & s_{vv} \end{bmatrix} \begin{bmatrix} F_{hh} & 0 \\ F_{vh} & F_{vv} \end{bmatrix} \begin{bmatrix} 1 \\ 0 \end{bmatrix} \tag{32}$$

Depending on the exact hardware source of cross-polar power, the mathematical models may differ. The proposed experiment validates the robustness of eigenvalue signal processing with respect to coaxial cross-polarization on transmit in radars with parabolic reflector antennas. The effects of antenna cross-coupling on transmit are the most relevant, since SU(2) transformations of the Coherency matrix do exactly correspond to a change of the receive polarization basis, and therefore the invariance of eigenvalue-derived variables with respect to cross-channel coupling on receive is mathematically exact.

In the acquired PPIs (Fig. 4) considerable blockage occurs in the western sector, and interference appears as radial lines and arcs throughout the rest of the PPI disc. Radials for the analysis were chosen at azimuth angle of 352°, where the microwave ray only goes through light rain (from 10 to 40 km) and the melting band (from 45 to 60 km), but avoids more complex scattering situations like ground clutter (visible at around 25 km from the radar in the NE sector) and electromagnetic interference.

In the following paragraph A, we analyze the effects of eigenvalue signal processing on the cc-off hardware configuration. In the cc-off configuration, in light rain, the antenna yields slightly high values of LDR (~ -26 dB) and low values of $\rho_{xh}$ (~ 0.2 - 0.3), indicating that a certain amount of incoherent cross-polar power is present. In this case, the bias reduction in polarimetric variables given by ESP is minimal. In fig. 5, blue curves refer to the cc-off/ESP-off configuration, whereas green curves refer to the cc-off/ESP-on configuration. Besides confirming that incoherent cross-polar power cannot be effectively removed by ESP, the results of paragraph A, reported in Fig. 5 and 6, confirm the theoretical inequalities of (15), (18) and (20).

In the following paragraph B we compare the cc-off/ESP-off configuration (blue curves) with the cc-on/ESP-on and with the cc-on/ESP-off configurations (red curves). In the cc-on configuration cross-polar isolation is significantly lowered (LDR in light rain is about -21 dB), but the additional cross-polar power is coherent, as indicated by the higher cross-polar correlation coefficient ($\rho_{xh}$ ~ 0.8) and the bias in polarimetric varables is effectively removed by ESP (Fig. 7).

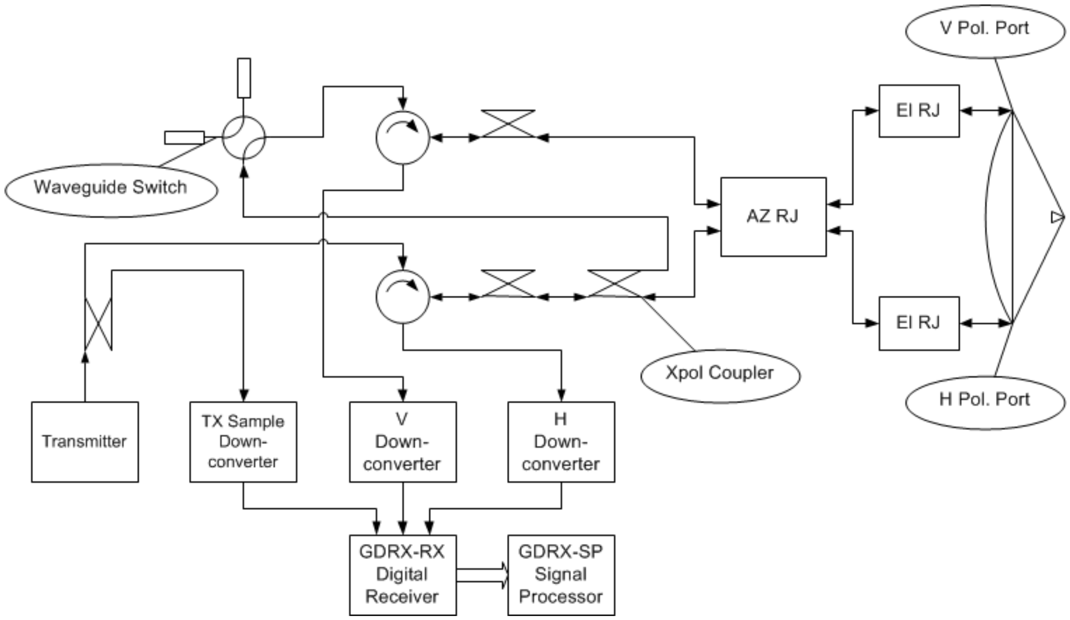


**Fig. 3** Radar system block diagram for the cross-coupling on (cc-on) configuration. A 20 dB waveguide coupler (Xpol Coupler) extracts power from the H Tx waveguide and feeds it to the V Tx waveguide.

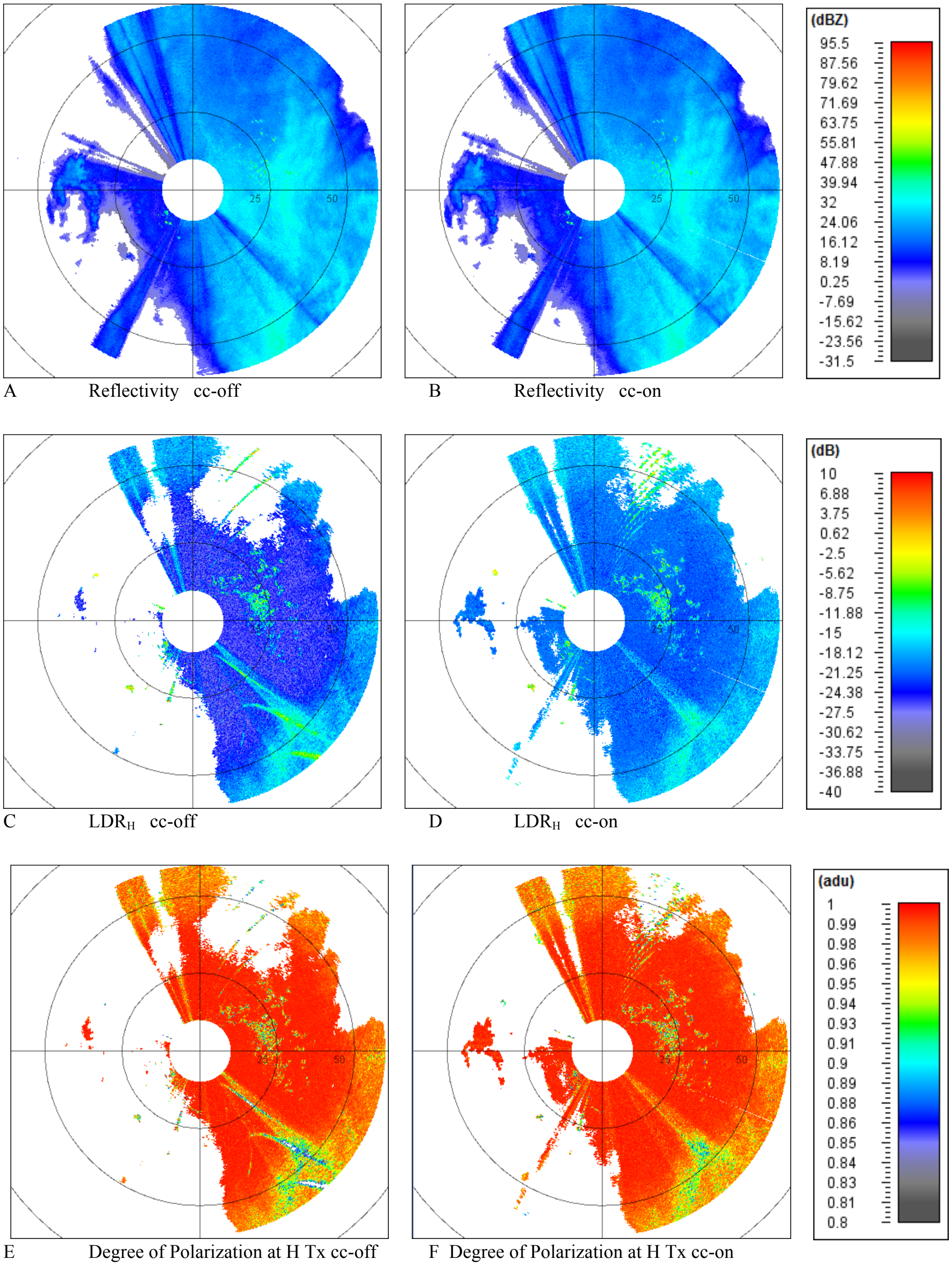


**Fig. 4** Panels from A to F are PPIs at 1.5˚ elevation of polarimetric variables at LDR mode. The black circles indicate ranges of 25, 50 and 75 km respectively. The PPIs on the left (Panels A, C and E) correspond to data acquired in the cross-coupling off (cc-off) configuration; the PPIs on the right (Panels B, D and F) correspond to data acquired in the cross-coupling on (cc-on) configuration. Rain is present between 10 and 50 km from the radar, the melting band appears as a low $LDR_H/DOP_H$ ring beyond 50 km. Beam blockage is present in the western quadrants, clutter is present mainly in the first quadrant at about 25 km range. Interference appears as low $LDR_H/DOP_H$ lines/arcs and changes characteristics between the two acquisitions (spaced in time 1.5 minutes). Copolar reflectivity is not significantly affected by coupling. $LDR_H$ is affected by coupling, and good isolation (panel C) enhances the contrast between rain and the melting band with respect to poor isolation (panel D). $LDR_{H\_ESP}$ (not reported for compactness) is identical to $LDR_H$ cc-off (panel C) and does recover the unbiased $LDR_H$ field as shown in Fig. 7E. Finally, $DOP_H$ is invariant with respect to cross-channel coupling, as can be qualitatively assessed by panels E and F of Fig.4, and further analyzed in Fig. 7F. For the quantitative analysis, we select a radial at 352˚ azimuth, where only rain and wet aggregates (melting band) are present.

*A. ESP for* the *cc-off configuration*

The values of $LDR_H$ and $\rho_{xh}$ in drizzle/light rain provide a comprehensive characterization of the coherent and incoherent cross-polar power radiated by the antenna, as explained in [1]. In particular, the cross-polar correlation coefficient $\rho_{xh}$ provides a measurement of coherent cross-polar power (equation (66) in [1]).

In the cc-off configuration, the antenna is characterized by intrinsic $\rho_{xh}$ equal to about 0.3 (blue curve in Fig. 7C). We therefore apply ESP to the cc-off configuration to find that eigenvalue-derived variables (ESP-on) differ slightly from their standard (ESP-off) counterparts (Fig. 5), as predicted by the theory of Section II. In the following, we seek experimental proof of the inequalities in (15), (18) and (20). For the cc-off configuration, the difference between $Z_{VH}$ and $Z_{VH\_ESP}$ and between $LDR_H$ and $LDR_{H\_ESP}$ is visible (Fig. 5 B-C), whereas the difference between $Z_{HH}$ and $Z_{HH\_ESP}$ is not noticeable (Fig. 5A). In table III, mean and standard deviation of 101 data points between 15 and 30 km (light rain) are reported and do confirm the inequalities in (15) and (20). To ascertain the validity of the inequality in (18), we resorted to consider both cc-off and cc-on configurations, and we reported the differences between $Z_{HH\_ESP}$ and $Z_{HH}$ in Fig. 6. We note how $Z_{HH\_ESP} > Z_{HH}$ in the cc-on configuration, and how the difference between ESP and traditional variables grows larger for increasing levels of coherent cross-channel coupling (Fig. 6 and 7). With reference to Fig. 6, we averaged 101 data points between 15 and 30 km from the radar (light rain), where the bias induced in copolar reflectivity $Z_{HH}$ (specifically $Z_{HH\_ESP}$ - $Z_{HH}$ for the cc-on configuration, Fig. 6B) is 0.02241 dBZ. Equation (16) of Section II, the trace invariance for SU(2) transformations, links the bias in copolar reflectivity $Z_{HH}$ to the bias in linear depolarization ratio $LDR_H$ with the formula

$$\frac{Z_{HH\_ESP}}{Z_{HH}} = \frac{1 + LDR_H}{1 + LDR_{H\_ESP}} \qquad (33)$$

We will see in paragraph B that the difference between $LDR_H$ and $LDR_{H\_ESP}$ (fig. 7D and 7E) for the cc-on configuration for the same data points between 15 and 30 km is 4.82 dB, that, injested in equation (33), yields a predicted bias in copolar reflectivity of 0.02238 dB, in perfect agreement with the bias in copolar reflectivity $Z_{HH}$ experimentally observed in Fig. 6B. We conclude that

- For antennas where incoherent cross-polar power is dominant ($\rho_{xh}$ in drizzle/light rain is less than about 0.3), ESP does not substantially improve the quality of the measurements, as theoretically demonstrated in [1] for $DOP_H$.
- The inequalities in (15), (18) and (20) are experimentally verified.
- Formula (33) provides an accurate relation between the bias in $Z_{HH}$ and the bias in $LDR_H$.
- The difference between standard and ESP variables grows larger for increasing levels of <u>coherent</u> antenna cross-channel coupling.

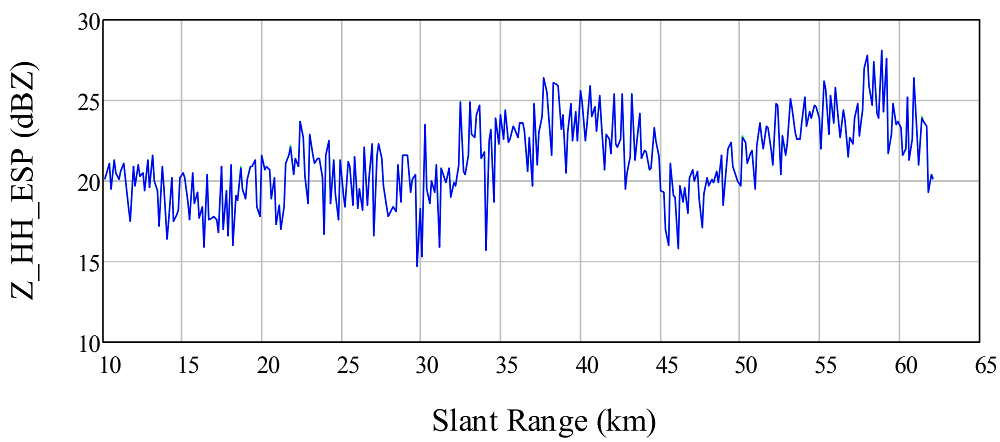


A Copolar reflectivity ESP-off ($Z_{HH}$, blue curve) and copolar reflectivity ESP-on ($Z_{HH\_ESP}$ green curve) for the cc-off configuration. With $\rho_{xh}$ equal to about 0.3 (Fig. 7C, blue curve), the application of ESP does not significanlty affect copolar reflectivity, and the blue and green curves are perfectly superimposed.

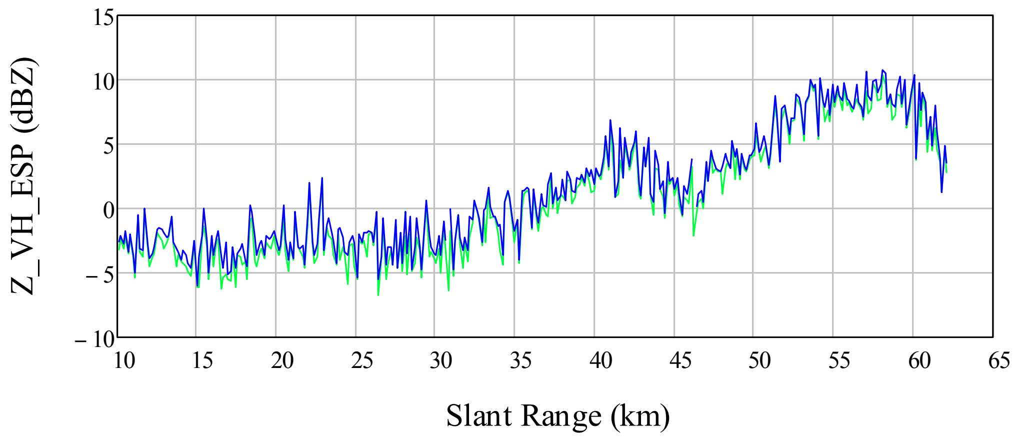


B Cross-polar reflectivity ESP-off ($Z_{VH}$, blue curve) and cross-polar reflectivity ESP-on ($Z_{VH\_ESP}$ green curve) for the cc-off configuration. The application of ESP lowers cross-polar reflectivity as predicted in formula (20).

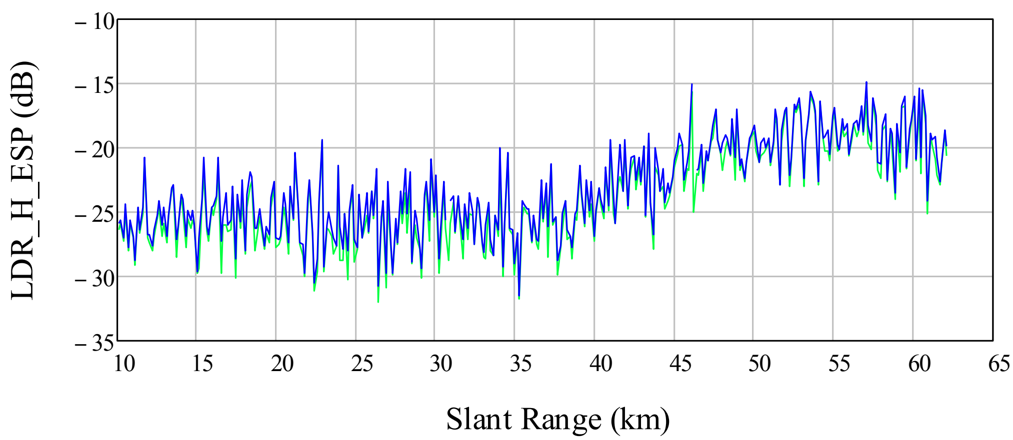


C Linear Depolarization Ratio ESP-off (LDR, blue curve) and Linear Depolarization Ratio ESP-on ($LDR_{H\_ESP}$ green curve) for the cc-off configuration. The application of ESP lowers the Linear Depolarization Ratio as predicted in formula (15).

**Fig. 5** Comparison of ESP-on and ESP-off versions of $Z_{HH}$, $Z_{VH}$ and $LDR_H$ for the cc-off configuration. Even with relatively low coherent cross-channel coupling ($\rho_{xh}$ is about 0.3 for the cc-off configuration) ESP produces slight changes in $Z_{VH}$ and $LDR_H$, in agreement with the theory of Section II.

TABLE III. AVERAGED DATA POINTS BETWEEN 15 AND 30 KM (LIGHT RAIN) FOR CC-OFF

| | ***Mean*** | ***Standard Deviation*** |
|---|---|---|
| $Z_{HH}$ | 19.62 dBZ | 1.86 dBZ |
| $Z_{HH\_ESP}$ | 19.62 dBZ | 1.86 dBZ |
| $Z_{VH}$ | -2.61 dBZ | 1.58 dBZ |
| $Z_{VH\_ESP}$ | -3.31 dBZ | 1.66 dBZ |
| $LDR_H$ | -25.35 dB | 2.48 dB |
| $LDR_{H\_ESP}$ | -26.05 dB | 2.56 dB |

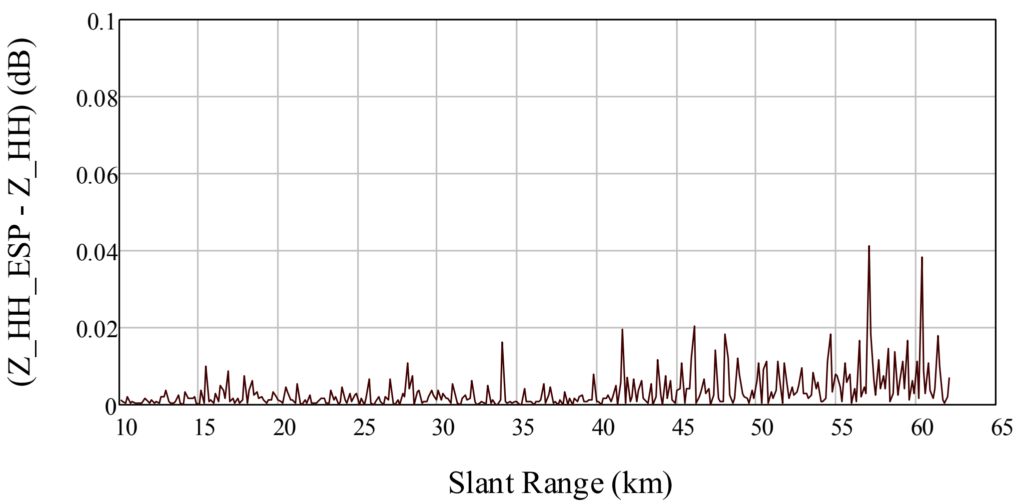


A Difference between $Z_{HH\_ESP}$ and $Z_{HH}$ is negligible for the cc-off configuration ($\rho_{xh} \sim 0.3$).

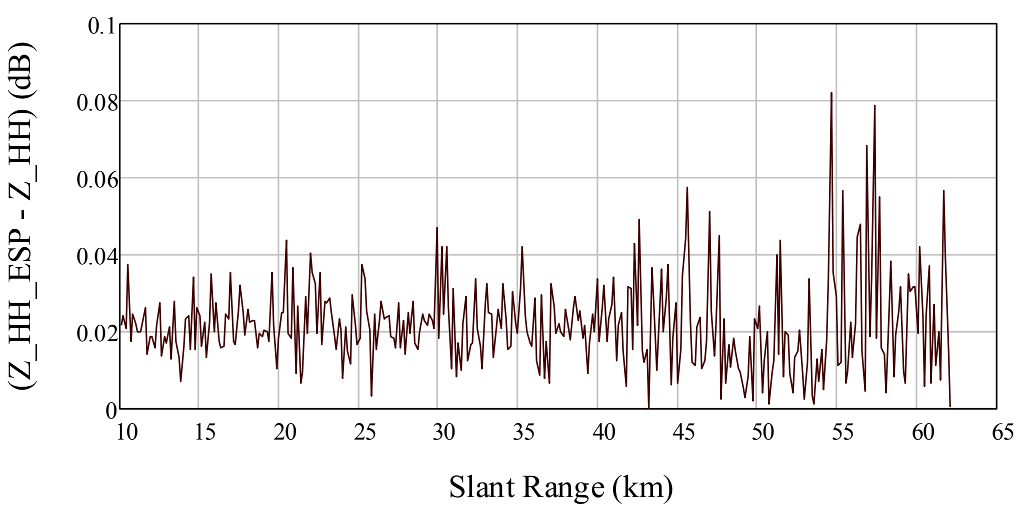


B Difference between $Z_{HH\_ESP}$ and $Z_{HH}$ is larger for the cc-on configuration ($\rho_{xh} \sim 0.8$).

**Fig. 6** Difference between $Z_{HH\_ESP}$ and $Z_{HH}$ for the cc-off (A) and cc-on (B) configurations. Between 15 and 30 km, the bias of 0.022 dBZ in copolar reflectivity $Z_{HH}$ showed in 6B is in excellent agreement with the bias in $LDR_H$ of 4.82 dB in Fig 7D. In general, for increasing antenna coherent cross-channel coupling, the difference between ESP and standard variables becomes larger.

*B. Comparison between cc-off and cc-on configurations*

We now compare results from the cc-off and cc-on configurations to experimentally prove the theoretical results of Section II.

The cross-polar correlation coefficient $\rho_{xh}$ in drizzle/light rain represents the amount of coherent cross-channel coupling (equation (66) in [1]). Fig. 7C shows that, in drizzle/light rain between 15 and 30 km, for the cc-off configuration the antenna yields values of $\rho_{xh}$ around 0.3, whereas for the cc-on configuration the antenna yields values around 0.8. In agreement with the theory, coherent cross-channel coupling (induced by the cc-on configuration) increases the measured cross-polar correlation coefficient.

In Fig. 7A, standard (ESP-off) cross-polar reflectivity ($Z_{VH}$) from the cc-on (red curve) and cc-off (blue curve) configurations are compared. We can observe that cross-channel coupling (induced by the cc-on configuration) increases cross-polar reflectivity.

In Fig. 7B, Eigenvalue Signal Processing is applied to data collected in the cc-on configuration (red curve), and compared to standard (ESP-off) cross-polar reflectivity from the cc-off configuration (blue curve in Fig. 5B is the same as in Fig. 7A). We can observe that ESP lowers cross-polar reflectivity to values comparable to, or lower than those corresponding to the ESP-off/cc-off configuration. This is in accordance with the theory. Specifically, ESP-corrected cross-polar reflectivity ($Z_{VH\_ESP}$, that is, the smallest eigenvalue) is lower than standard (ESP-off) cross-polar reflectivity from the cc-off configuration ($Z_{VH}$) because, even in the cc-off configuration, some residual coherent cross-channel coupling is present ($\rho_{xh} \sim 0.3$ in Fig. 7C, blue curve).

Fig. 7D contains standard (ESP-off) $LDR_H$ from the cc-on (red curve) and cc-off (blue curve) configurations. It can be observed that cross-channel coupling increases $LDR_H$ by a significant amount. Such increase is more visible in weakly depolarizing scatterers like light rain, and less visible in the melting band. We also note how the dynamic range of $LDR_H$ is reduced by increased cross-channel coupling, and therefore poor antenna isolation reduces the polarimetric contrast between different target types, making discrimination more difficult. For example, applications like supercooled droplets detection, where LDR has shown some discrimination capabilities, require high antenna polarimetric purity.

Fig. 7E shows that application of ESP to data acquired in the cc-on configuration ($LDR_{H\_ESP}$) retrieves values almost identical to the cc-off configuration. Note that not only ESP lowers the minimum LDR, but also restores the dynamic range corresponding to the cc-off configuration.

We also proceeded to a more quantitative analysis of 101 data points between 15 and 30 km (light rain), for which the mean $LDR_{H\_ESP}$ (from cc-on) is -25.94 dB, whereas the mean $LDR_H$ from the cc-off configuration is -25.35 dB (difference is 0.59 dB). This is in agreement with the theory, predicting $LDR_{H\_ESP} \leq LDR_H$. The standard deviation for $LDR_H$ cc-off was 2.48 dB and for $LDR_{H\_ESP}$ was 2.4 dB. This latter measurement suggests that ESP variables (that indirectly incorporate the noisy cross-polar correlation coefficient) are not affected more by noise than their standard counterparts. The mean $LDR_H$ for the cc-on configuration (ESP-off) was -21.12 dB with a standard deviation of 1.42 dB. For this particular antenna, in light rain between 15 and 30 km, application of ESP expands the dynamic range of the depolarization ratio by 4.82 dB, in perfect agreement with the bias of 0.022 dBZ in copolar refelctivity observed in Fig. 6B. Increased cross-channel coupling reduces the dynamic range and lowers the statistical noise of the depolarization ratio.

Fig. 7F gives an experimental proof of the concepts exposed in [1] and shows that the Degree of Polarization at horizontal transmit $DOP_H$ is very robust with respect to antenna cross-channel coupling.

It should be noted that ESP theory assumes target reflection symmetry and, under such assumption, $LDR_{H\_ESP}$ and $DOP_H$ are one-to-one related, and therefore these two variables contain the same information.

The ESP experiment permits to conclude that eigenvalue-derived variables ($Z_{HH\_ESP} \equiv \lambda_{H1}$, $Z_{VH\_ESP} \equiv \lambda_{H2}$, $LDR_{H\_ESP} \equiv \lambda_{H2}/\lambda_{H1}$, $DOP_H = (\lambda_{H1}-\lambda_{H2})/(\lambda_{H1}+\lambda_{H2})$) are robust with respect to antenna cross-channel coupling, whereas standard variables ($Z_{HH} \equiv <|s_{hh}|^2>$, $Z_{VH} \equiv <|s_{vh}|^2>$, $LDR_H \equiv <|s_{vh}|^2>/<|s_{hh}|^2>$), simply derived from the entries of the Coherency matrix, are not.

Eigenvalue Signal Processing provides an accurate mathematical framework for the quantitative analysis of the bias induced by antenna coherent and incoherent cross-channel coupling in polarimetric weather radar variables, and permits the retrieval of polarimetric variables ($Z_{HH}$ and $LDR_H$) unbiased by coherent cross-channel coupling. Any biased induced by incoherent cross-channel coupling will still be present in the ESP estimates.

Experimental analysis of the bias in differential reflectivity $Z_{DR}$ will be deferred to a subsequent paper, where the fully polarimetric aspects of Eigenvalue Signal Processing will be analyzed.

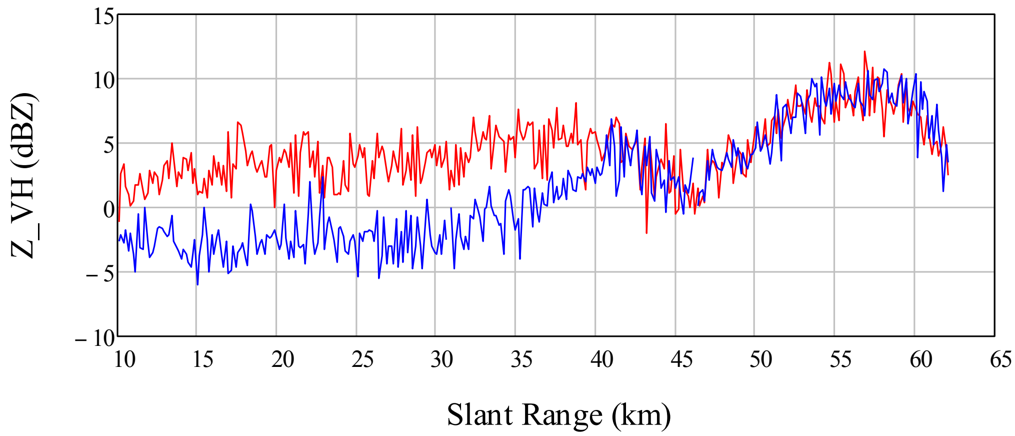


A Standard Cross-polar Reflectivity $Z_{VH}$ (ESP-off) for the cc-off (blue) and cc-on (red) configurations. Cross-channel coupling (cc-on, red curve) increases cross-polar reflectivity with respect to the cc-off configuration. This phenomenon is well visible in rain, between 10 and 40 km and less visible in the melting band (50-60 km).

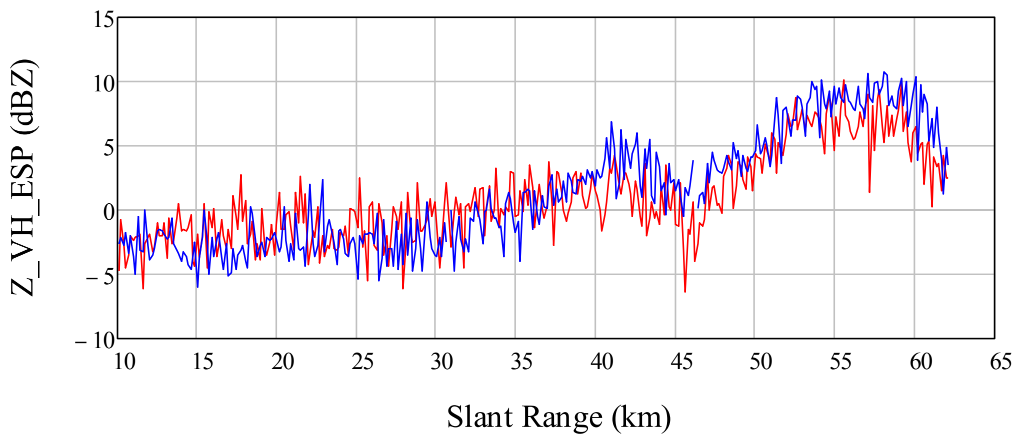


B Standard Cross-polar Reflectivity $Z_{VH}$ (dBZ) for the cc-off configuration as in A (blue curve), superimposed with ESP-corrected cross-polar reflectivity (smallest eigenvalue) obtained from the cc-on configuration: $Z_{VH\_ESP}$ (red curve). By comparing A and B we can observe that Eigenvalue Signal Processing lowers cross-polar refelctivity in rain (10-40 km) and in the melting band (50-60 km) to levels comparable with or below the cc-off configuration, as predicted by the theory. Note how ESP increases the overall dynamic range of $Z_{VH}$.

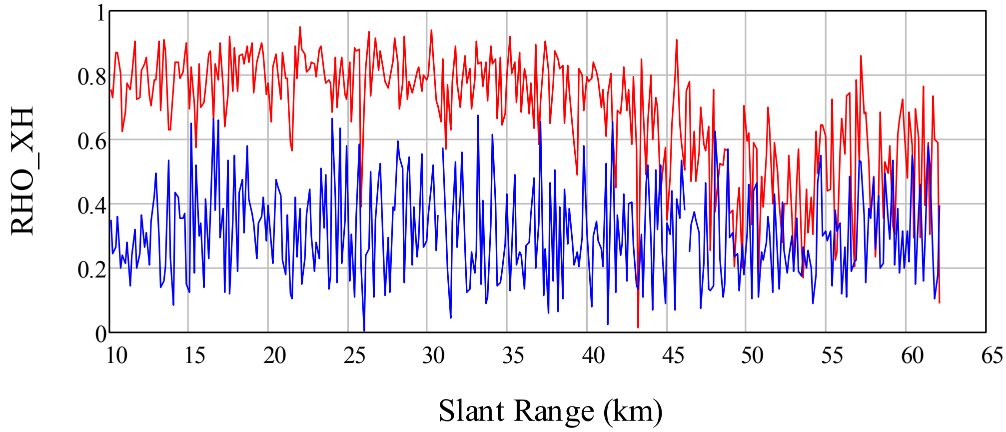


C Cross-polar Correlation coefficient $\rho_{xh}$. The cross-polar correlation coefficient provides a measurement of antenna coherent cross-channel coupling. The red curve refers to the cc-on configuration (high $\rho_{xh}$), the blue curve refers to the cc-off configuration (low $\rho_{xh}$).

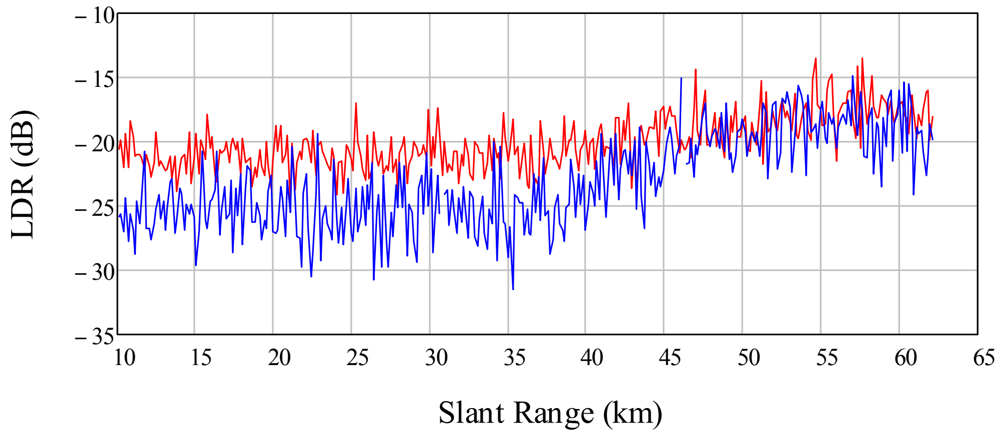


D Linear Depolarization Ratio (dB). $LDR_H$ is affected by antenna coupling as it is clearly illustrated by the red curve (standard $LDR_H$ corresponding to cc-on) and blue curve, (standard $LDR_H$ corresponding to cc-off). The difference is blurred after 45 km, where more depolarizing scatterers (melting band) are present, and the effects of imperfect isolation become less visible. Lack of polarimetric purity decreases the polarimetric contrast and makes discrimination more difficult.

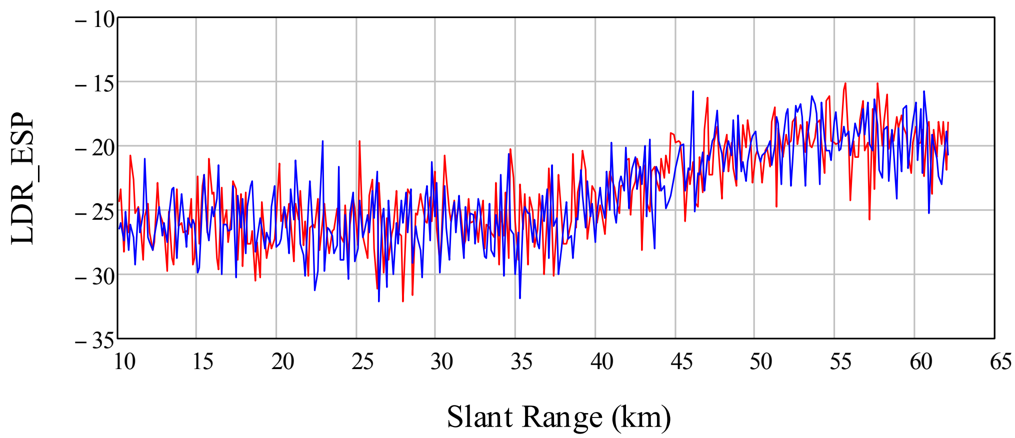


E Linear Depolarization Ratio (dB). Blue curve is standard $LDR_H$ for the cc-off configuration (same as blue curve in D), red curve is ESP-corrected LDR ($LDR_{H\_ESP}$) from the cc-on configuration. Eigenvalue Signal Processing recovers the unbiased $LDR_H$ (red curve superimposes with the blue curve) and restores the dynamic range corresponding to the cc-off configuration. In general, $LDR_{H\_ESP} \leq LDR_H$. Equality holds for an antenna with no coherent cross-channel coupling.

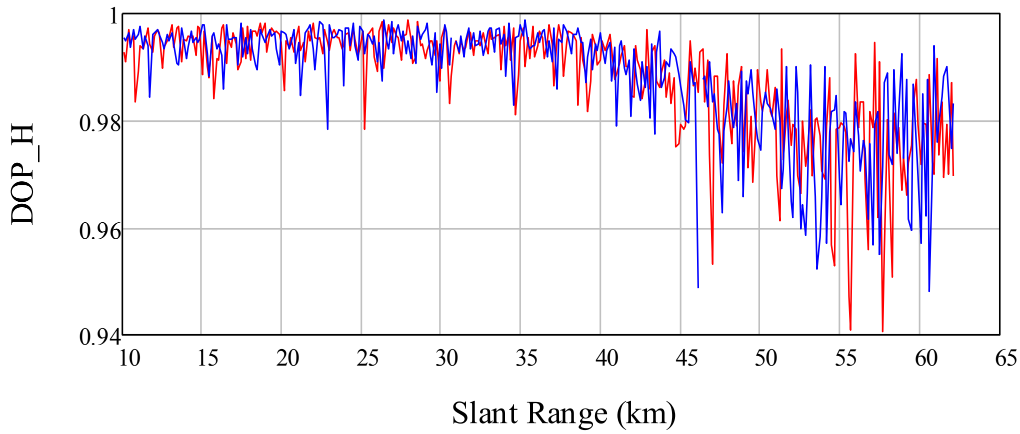


F Degree of Polarization at Horizontal transmit ($DOP_H$). The degree of polarization at horizontal transmit can be expressed in terms of the eigenvalues of the Coherency matrix, and is therefore invariant with respect to antenna cross-channel coupling, as clearly indicated by the superimposed red and blue curves corresponding to the cc-on and cc-off configurations respectively.

**Fig. 7** Radial plots for 352˚ azimuth (between 352˚ and 352.5˚). The radial goes through rain (10-40 km) and then through the melting band (> 40km). The word "standard" refers to standard signal processing (ESP-off), the term "ESP-corrected" refers to the eigenvalue-derived variables (ESP-on). In the panels from A to F, standard polarimetric variables from the cc-off configuration (blue curves) are compared with standard and ESP-corrected poarimetric variables from the cc-on configuration (red curves).

## IV. CONCLUSIONS

Eigenvalue Signal Processing is a novel polarimetric signal processing procedure that permits the removal of the bias induced by antenna coherent cross-polar power in weather radar variables, specifically in reflectivity Z, differential reflectivity $Z_{DR}$ and linear depolarization ratio LDR. It is applicable in polarimetric weather radars operating at LDR, ATSR and STSR orthogonal modes. It is not applicable at STSR hybrid mode, since it requires orthogonal polarization bases. The strength of the approach is that bias correction is effected automatically by means of the diagonalization of the Coherency matrices at horizontal and vertical polarizations, and knowledge of the actual amount of cross-polar power radiated by the antenna is not necessary.

ESP is effective for the removal of the biases induced by coherent cross-polar power (coaxially radiated cross-polar power) but cannot remove the biases due to incoherent cross-polar power (radiated as a quad of offset lobes). Consequently, the effectiveness of the ESP technique is dependent on the spatial structure of cross-polar power and therefore varies from antenna to antenna. For example, the improvement in LDR, in the case reported in the present paper (Gematronik METEOR 600C), is of about 5 dB. Tests performed at Prosensing Inc. on a Ka-band polarimetric radar showed improvements in LDR of about 7 dB (will be reported in an upcoming paper).

In this paper, the theory of Eigenvalue Signal Processing was experimentally tested at LDR mode with good results for copolar reflectivity $Z_{HH}$, cross-polar reflectivity $Z_{VH}$, Linear Depolarization Ratio $LDR_H$ and Degree of Polarization $DOP_H$. In particular, it is demonstrated that ESP can recover the unbiased LDR, named $LDR_{ESP}$, with the dynamic range corresponding to an antenna solely affected by incoherent cross-polar power. The robustness with respect to coherent antenna cross-channel coupling of the degree of polarization at horizontal transmit $DOP_H$ is experimentally proven, as theoretically analyzed in [1]. Under the assumption of reflection symmetry, $LDR_{ESP}$ and $DOP_H$ are one-to-one related, and therefore contain the same information. Use of eigenvalue-derived variables is recommended to enhance the polarimetric performance of radars at LDR, ATSR and STSR orthogonal modes in presence of parabolic reflector antennas with imperfect polarimetric isolation. Ongoing work involves experimental testing with planar phased-array antennas and will also consider the fully polarimetric aspects of eigenvalue signal processing, specifically the retrieval of antenna unbiased estimates of differential reflectivity $Z_{DR\_ESP}$.

REFERENCES


[1] Galletti, M.; Zrnic, D.S.; Melnikov, V.M.; Doviak, R.J., "Degree of Polarization at Horizontal Transmit: Theory and Applications for Weather Radar," Geoscience and Remote Sensing, IEEE Transactions on , vol.50, no.4, pp.1291,1301, April 2012

[2] Nghiem, S. V., Yueh, S.H., Kwok, R., and Li, F.K. Symmetry properties in polarimetric remote sensing. Radio Sci., 27: 693-711, 1992.

[3] Zahrai, A.; Zrnic, D., "Implementation of polarimetric capability for the WSR-88D (NEXRAD) radar," Aerospace and Electronics Conference, 1997. NAECON 1997., Proceedings of the IEEE 1997 National , vol.1, no., pp.346,352 vol.1, 14-18 Jul 1997

[4] Bebbington, D.; Carrea, L., "Geometric Polarimetry—Part I: Spinors and Wave States," Geoscience and Remote Sensing, IEEE Transactions on , vol.PP, no.99, pp.1,16, 0.

[5] Graves, C. D., "Radar Polarization Power Scattering Matrix," Proceedings of the IRE , vol.44, no.2, pp.248,252, Feb. 1956

[6] Kwiatkowski, John M., Alexander B. Kostinski, A. R. Jameson, 1995: The Use of Optimal Polarizations for Studying the Microphysics of Precipitation: Nonattenuating Wavelengths. *J. Atmos. Oceanic Technol.*, **12**, 96–114.

[7] Cloude, S.R.; Pottier, E., "A review of target decomposition theorems in radar polarimetry," Geoscience and Remote Sensing, IEEE Transactions on , vol.34, no.2, pp.498,518, Mar 1996

[8] J.-S. Lee and E. Pottier, Polarimetric Radar Imaging: From Basics to Applications. Boca Raton, FL:CRC Press, 2009

[9] Baum, Kritikos editors, "Electromagnetic Symmetry" - Chapter 2 "Lie Groups in electromagnetic wave propagation and scattering" Shane R. Cloude.

[10] M. Galletti, D. H. O. Bebbington, M. Chandra, T. Boerner, "Measurement and Characterization of Entropy and Degree of Polarization of Weather Radar Targets," *IEEE Transactions on Geoscience and Remote Sensing*, vol. 46, no. 10, pp. 3196-3207, October 2008.

[11] Galletti, M.; Chandra, M.; Borner, T.; Bebbington, D. H O, "Degree of polarization for weather radars," Geoscience and Remote Sensing Symposium, 2007. IGARSS 2007. IEEE International , vol., no., pp.4187,4190, 23-28 July 2007

[12] Giuli, D.; Fossi, M.; Facheris, L., "Radar target scattering matrix measurement through orthogonal signals," Radar and Signal Processing, IEE Proceedings F , vol.140, no.4, pp.233,242, Aug 1993.

[13] Giuli, D.; Facheris, L.; Fossi, M.; Rossettini, A., "Simultaneous scattering matrix measurement through signal coding," Radar Conference, 1990., Record of the IEEE 1990 International , vol., no., pp.258,262, 7-10 May 1990.

[14] Chandrasekar, V., and Nitin Bharadwaj. "Orthogonal channel coding for simultaneous co-and cross-polarization measurements." Journal of Atmospheric and Oceanic Technology 26.1 (2009): 45-56.

[15] Y. Wang and V. Chandrasekar, "Polarization isolation requirements for linear dual-polarization weather radar in simultaneous transmission mode of operation" *IEEE Transactions on Geoscience and Remote Sensing*, vol. 44, no. 8, pp. 2019-2028, August 2006.

[16] Mueller, E. A. "Calculation procedures for differential propagation phase shift." In Conference on Radar Meteorology, 22nd, Zurich, Switzerland, pp. 397-399. 1984.

[17] V. N. Bringi and V. Chandrasekhar, *Polarimetric Doppler Weather Radar. Principles and applications*, Cambridge University Press, 2001.

[18] D. S. Zrnic, R. J. Doviak, G. Zhang and A. Ryzhkov, "Bias in differential reflectivity due to cross-coupling through radiation patterns of polarimetric weather radars " J. Atmos. Ocean. Technol., 27, 1624-1637, 2010.

[19] G. Zhang, R.J. Doviak, D.S.Zrnic, J. Crain, D. Staiman, Y. Al-Rashid, "Phased Array Radar Polarimetry for Weather Sensing: a Theoretical Formulation for Bias Correction", IEEE Transactions on Geoscience and Remote Sensing, vol. 47, no. 11, Nov. 2009.

[20] Bringi, V. N., R. Hoferer, D. A. Brunkow, R. Schwerdtfeger, V. Chandrasekar, S. A. Rutledge, J. George, P. C. Kennedy, 2011: Design and Performance Characteristics of the New 8.5-m Dual-Offset Gregorian Antenna for the CSU–CHILL Radar. J. Atmos. Oceanic Technol., 28, 907–920.

[21] Galletti, Zrnic, Melnikov, Doviak, "Degree of Polarization: Theory and Applications for Weather Radar at LDR mode", Proceedings of the 2011 IEEE Radar Conference, 23-27 May 2011, Kansas City, MO.

[22] R. J. Doviak and D. S. Zrnic, *Doppler Radar and Weather Observations*, 2nd ed. San Diego, CA: Academic Press, 1993.

[23] E. Wolf, "Coherence Properties of Partially Polarized Electromagnetic Radiation", Il Nuovo Cimento, Vol. XIII, N. 6, 16 Settembre 1959, pp. 1165-1181.

[24] M. Born and E. Wolf, *Principles of Optics:Electromagnetic Theory of Propagation, Interference and Diffraction of Light,* 7th ed. Cambridge, UK: Cambridge Univ. Press, 1999.

[25] https://maps.google.com/maps?q=Selex+Systems+Integration+GmbH,+Raiffeisenstra%C3%9Fe,+Neuss,+Germany&hl=en&ie=UTF8&ll=51.131554,6.735869&spn=0.001171,0.003575&sll=40.906488,-72.884172&sspn=0.180595,0.457649&oq=Selex+systems+inte&t=h&z=19

[26] http://www.gematronik.com/products/radar-systems/meteor-600c-635c/

[27] http://www.gematronik.com/fileadmin/media/pdf/ProductDatasheet/METEOR_600C-635C_engl_1907154815.pdf

[28] D. Moisseev, C. Unal, H. Russchemberg, L. Ligthart, "A New Method to Separate Ground Clutter and Atmospheric Reflections in the Case of Similar Doppler Velocities", Transactions on Geoscience and Remote Sensing, Vol. 40 n. 2, February 2002.

[29] Michele Galletti, "Fully Polarimetric Analysis of Weather Radar Signatures", Ph.D. Thesis, available at http://www.dart-europe.eu/full.php?id=257943

[30] M. Galletti, D. H. O. Bebbington, M. Chandra, T. Boerner, "Fully polarimetric analysis of weather radar signatures" Proc. 2008 IEEE Radar Conference, Rome, Italy, May 2008.

[31] M. Galletti, D. Zrnic, R. Doviak, G. Zhang, "Polarimetric Phased Array Weather Radar: Concepts for Polarimetric Calibration" Proc. 2010 IEEE Phased Array Conference, Boston MA, October 2010.

[32] M. Galletti, D. Zrnic, "Bias in Copolar Correlation Coefficient caused by Antenna Radiation Patters" IEEE Transactions on Geoscience and Remote Sensing, 2011.

[33] A. Ryzhkov, D. S. Zrnic, J. C. Hubbert, Bringi V. N., Vivekanandan J., Brandes Edward A., "Polarimetric radar observations and interpretation of co-cross-polar correlation coefficients", Journal of Atmospheric and Oceanic Technology, vol. 19, n.3 pp.340-354, 2002.

[34] Ryzhkov, A. V., "Interpretation of polarimetric radar covariance matrix for meteorological scatterers: Theoretical analysis", Journal of Atmospheric and Oceanic Technology, 18, 315-328, 2001.

[35] Fradin, A. Z., 1961: "Microwave antennas" Pergamon Press, London, UK, pp. 668.

[36] Valery M. Melnikov, "One-Lag Estimators for Cross-Polarization Measurements", Journal of Oceanic and Atmospheric Technology, 23 pp. 915-926 July 2006.

[37] Moisseev, D. N., C. M. H. Unal, H. W. J. Russchenberg and L. P. Ligthart, 2002: Improved polarimetric calibration for atmospheric radars. *J. Atmos. Oceanic Technol.,* 19 (12), 1968-1977 Moisseev